# Kinematics of charge transfer: $Ar^+ + H_2$

P. M. Hierl,* V. Pacák, and Z. Herman

*Czechoslovak Academy of Sciences, J. Heyrovsky Institute of Physical Chemistry and Electrochemistry, 121 38 Prague 2, Machova 7, Czechoslovakia*
(Received 22 November 1976)

Product angular and velocity vector distributions have been measured in a crossed beam experiment for the charge transfer process $Ar^+ + H_2 \rightarrow Ar + H_2^+$ at relative collision energies of 0.13, 0.48, and 3.44 eV. Charge transfer was found to occur by two distinct mechanisms: (1) a simple electron-jump mechanism which preserves the quasirectilinear trajectories of the colliding species and which selectively produces $H_2^+$ in the vibrational state most nearly resonant with the reactant ion, and (2) an intimate-collision mechanism which results in large-angle scattering and which produces $H_2^+$ in a broad range of vibrational states.

## I. INTRODUCTION

Because of the familiar problem of detecting very low (i.e., quasithermal) energy product ions, little direct experimental information exists on the collision dynamics of charge transfer processes at low collision energies. In a few cases, however, translational energy distributions have been measured[1-4] for the ionic products of electron transfer reactions. Recent studies in this laboratory have provided complete product contour maps (i.e., velocity and angular distributions) for two charge transfer reactions: (i) $Ar^+ + NO$, a system in which chemical reaction (atomic rearrangement) does not occur and in which charge transfer proceeds, in part, via the formation of a long-lived collision complex, particularly at the lowest collision energies[5(a)]; and (2) $Kr^+ + CH_4$, an essentially nonreactive system chemically, in which quasiresonant effects could be investigated because of the near continuum of internal states of the polyatomic product molecular ion.[5(b)]

As part of our continuing systematic investigation of the collision dynamics of charge transfer processes, we report here the results of a crossed beam experiment undertaken with two objectives: first, to determine the manner of energy disposal in an exothermic charge transfer process; second to investigate the competition between charge transfer and chemical reaction, particularly with regard to the frequently-made assumption[6] that, in a reactive system, intimate collisions lead exclusively to atomic rearrangement.

The charge transfer process

$$Ar^+ + H_2 \rightarrow Ar + H_2^+ \qquad (1)$$

was selected for this study. This system, in contrast to those previously studied, is very reactive chemically. In fact, the competing rearrangement process

$$Ar^+ + H_2 \rightarrow ArH^+ + H \qquad (2)$$

is one of the most thoroughly studied ion–molecule reactions.[7-18] There also exist data on the elastic[16] and inelastic[19] scattering at moderate collision energies (~3 eV), as well as theoretical calculations[20,21] based upon semiclassical trajectory methods. Finally, reaction (1) has the experimental advantages of a reasonably large cross section (~10 $A^2$[22,23]), large vibrational spacings in the product ion $H_2^+$ (0.26 eV),[24] and a favorable kinematic factor that allows low center-of-mass (c.m.) collision energies to be achieved.

An energy level diagram for the reactant and product ions is presented in Fig. 1. The recombination energy of $Ar^+$ in the $^2P_{3/2}$ ground state exceeds the vertical ionization potential of $H_2$ by 0.332 eV, an amount sufficient to produce $H_2^+$ in either the $v' = 0$ or the $v' = 1$ vibrational level. The $^2P_{1/2}$ state of $Ar^+$ lies 0.510 eV above ground state $H_2^+$, so the resulting $H_2^+$ product ion could contain as many as two quanta of vibrational energy. At the lowest collision energy ($T$) studied, 0.13 eV (c.m.), the total energy available is not sufficient to populate higher vibrational levels of $H_2^+$. At $T = 0.48$ eV, $H_2^+$ can be produced with as many as two quanta of vibrational energy from $Ar^+(^2P_{3/2})$ and four quanta from $Ar^+(^2P_{1/2})$. At the highest collision energy, 3.44

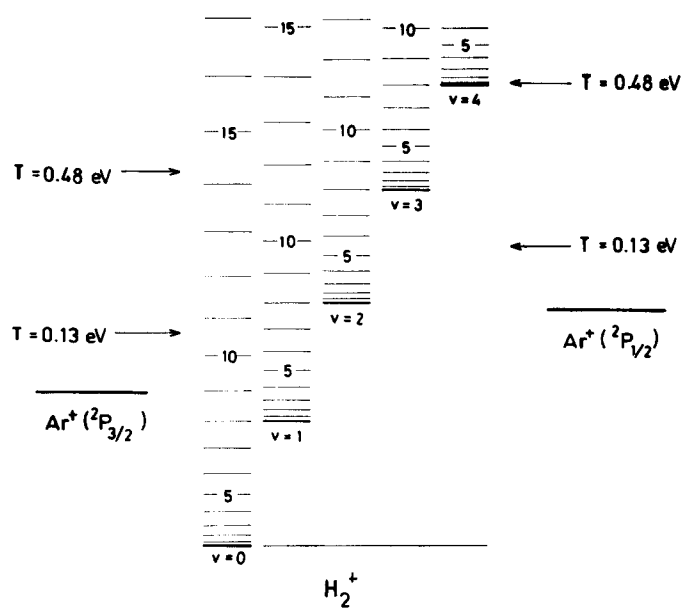


FIG. 1. Energy level diagram for the reactant $Ar^+$ in both the $^2P_{3/2}$ (left side of figure) and the $^2P_{1/2}$ (right side) states, relative to the $H_2^+$ product ion (center). Rotational levels of $H_2^+$ are indicated by light horizontal lines for the $v = 0$–4 vibrational states of $H_2^+$. Arrows indicate the total energy available in the experiments performed at $T = 0.13$ and 0.48 eV (c.m.). The internal energies of $H_2^+(v, J)$ were calculated from Ref. 24, and the ionization potentials of $H_2$ and Ar were obtained from Ref. 25.

 

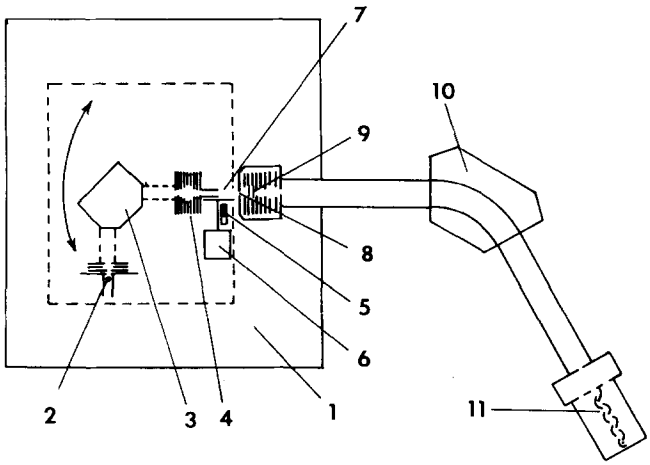


FIG. 2. Schematic diagram of the crossed beam instrument, EVA II. 1: vacuum chamber, 2: ion source, 3: primary mass selector, 4: deceleration lenses, 5: neutral beam source, 6: neutral beam chopper, 7: collision zone, 8; detection slit, 9: energy analyzer, 10: detection mass spectrometer, 11: electron multiplier.

eV, the total energy is sufficient to produce $H_2^+$ in vibrational states up to the dissociation limit.

Note that certain vibrational states of $H_2^+$ are in near resonance with $Ar^+$: the $v' = 1$ state lies 63 meV below $Ar^+(^2P_{3/2})$ and the $v' = 2$ state is only 13 meV below $Ar^+(^2P_{1/2})$. We shall refer to the formation of $H_2^+$ in these states as quasiresonant charge transfer (RCT), while formation of $H_2^+$ in higher vibrational states will be considered endothermic, as it requires translational to internal energy conversion. Likewise, formation of $H_2^+$ in lower vibrational states will be considered exothermic, as it requires internal to translational energy conversion.

## II. EXPERIMENTAL

Figure 2 presents a schematic diagram of the crossed-beam instrument, EVA II, used in this study. $Ar^+$ ions are produced by impact of 100 eV electrons and therefore are presumably distributed statistically in a 2:1 ratio between the $^2P_{3/2}$ and the $^2P_{1/2}$ states, which differ in energy by 0.178 eV.[25] After mass selection, these ions are decelerated and focused into a collimated, nearly monoenergetic beam. Usable beams with laboratory (LAB) energies as low as 0.5 eV are produced, typically, with an energy spread of 0.2 eV (FWHM) and an angular width of about 1° (FWHM). This ion beam is crossed at right angles by a modulated, thermal energy beam of $H_2$ molecules effusing from a multichannel capillary array. Angular distributions are measured by rotating the beams with respect to the fixed detector. Ions passing through the detection slit are energy analyzed by a retarding potential energy analyzer whose performance for low-energy ion detection has been carefully checked, mass analyzed by a 60° magnetic-sector mass spectrometer, and detected by an electron multiplier. Phase sensitive detection is used to distinguish reactions occurring in the crossed-beam region from those occurring in the background gas, and signal averaging is employed to enhance the signal-to-noise ratio.

Experiments were performed at relative collision energies of 3.44, 0.48, and 0.13 eV (c.m.), thus extending from moderate to near-thermal energies. In each case, laboratory angular distributions were measured by recording the ion intensity while rotating the beam sources with respect to the fixed detector. Laboratory energy distributions for the $H_2^+$ product ion were measured three times at each of ten to twenty discrete laboratory angles between −15° and +92°. These data, averaged and appropriately scaled at each angle, were used to construct contour maps of the product ion velocity vector distributions.[26] Finally, product c.m. angular and translational energy distributions were derived from these maps in accord with the usual transformation relations.[26]

## III. RESULTS

### A. Contour maps

Figure 3 shows the scattering contour diagram (Cartesian probabilities[26]) for $H_2^+$ produced in reaction (1) at the relative collision energy 3.44 eV (c.m.). The position of the center-of-mass serves as the origin, and the initial $H_2$ velocity in the c.m. defines the 0° direction. The line marked RCT shows the magnitude of the $H_2^+$ velocity expected if charge transfer occurs in a resonant manner; i.e., with no exchange between internal and translational energy. It can be seen that the product intensity peaks at or slightly beyond the RCT velocity and in the forward (0°) direction. In the c.m. system, this peak corresponds to $H_2^+$ ions which have experienced little or no angular deflection or kinetic energy change during the charge transfer process; in the LAB system, this peak corresponds to thermal energy $H_2^+$ ions. Note, however, that there is also a distinct ridge of very low product ion intensity at all angles. This large-angle scattering, which signifies appreciable momentum transfer during the charge transfer process, presumably arises from intimate encounters occuring in small impact parameter collisions.

The $H_2^+$ product velocity vector distribution produced at a relative collision energy of 0.48 eV is shown in Fig. 4. Although the main peak of product intensity is still in the forward direction and slightly beyond the RCT circle, the large-angle scattering has increased in importance and a distinct, secondary maximum has appeared in the backward (180°) direction. In contrast to the principal, forward maximum, this lower, back-scattered peak maximizes at product velocities less than the resonant velocity.

The results obtained at 0.13 eV relative collision energy are shown in Fig. 5. There is now even greater product intensity at large scattering angles, and the Cartesian intensity at the maximum of the back-scattered peak is greater than 70% of the maximum intensity of the forward-scattered peak. Comparison with Fig. 3 shows that decreasing the collision energy from 3.44 to 0.13 eV—a factor of 25—has caused the relative importance

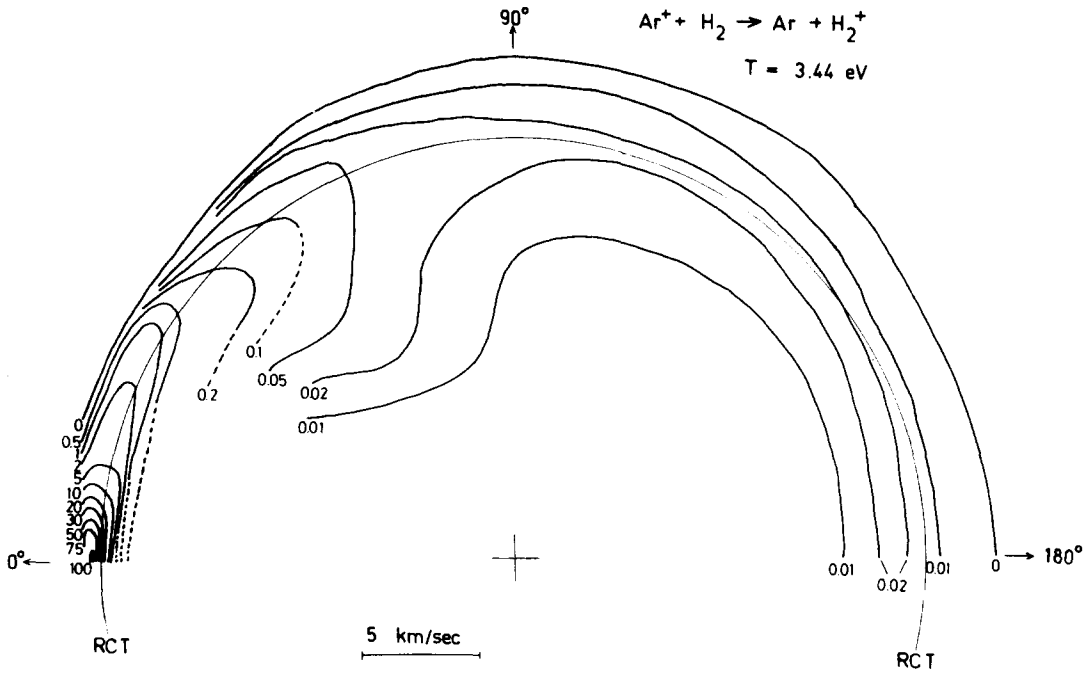


FIG. 3. Scattering contour map for $H_2^+$ produced in reaction (1) at the collision energy $T = 3.44$ eV (c.m.). The product ion intensities, normalized to 100 at the position of maximum intensity, are shown relative to the Cartesian system $P_C$. The position of the center-of-mass serves as the origin, and the initial $H_2$ velocity defines the 0° direction. The line marked RCT shows the magnitude of the $H_2^+$ velocity expected if charge transfer occurs in a resonant manner.

of the back-scattered peak to increase by a factor of about 3500.

Despite the nearly equal intensity in the forward and backward directions, however, note that the product distribution is not symmetric about the ± 90° axis, as would be required if the charge transfer process proceeded by the formation of an $ArH_2^+$ collision complex that had a lifetime greater than several rotational periods (about $10^{-13}$ sec). The forward-scattered $H_2^+$ ions peak at velocities slightly greater than the RCT velocity and are confined to c.m. scattering angles less than about 60°, whereas the back-scattered product ions peak at velocities considerably less than the RCT velocity and form a broad distribution extending over c.m. scattering angles from 60° to 180°. From this we conclude that reaction (1) occurs predominantly in a direct manner, with no evidence for the formation of a long-lived intermediate complex, over the energy range studied. Similar conclusions have been made for the rearrangement process, reaction (2).[12]

### B. c.m. angular distributions

Information on the reaction mechanism can be deduced from the c.m. angular distributions $I(\chi)$ which are

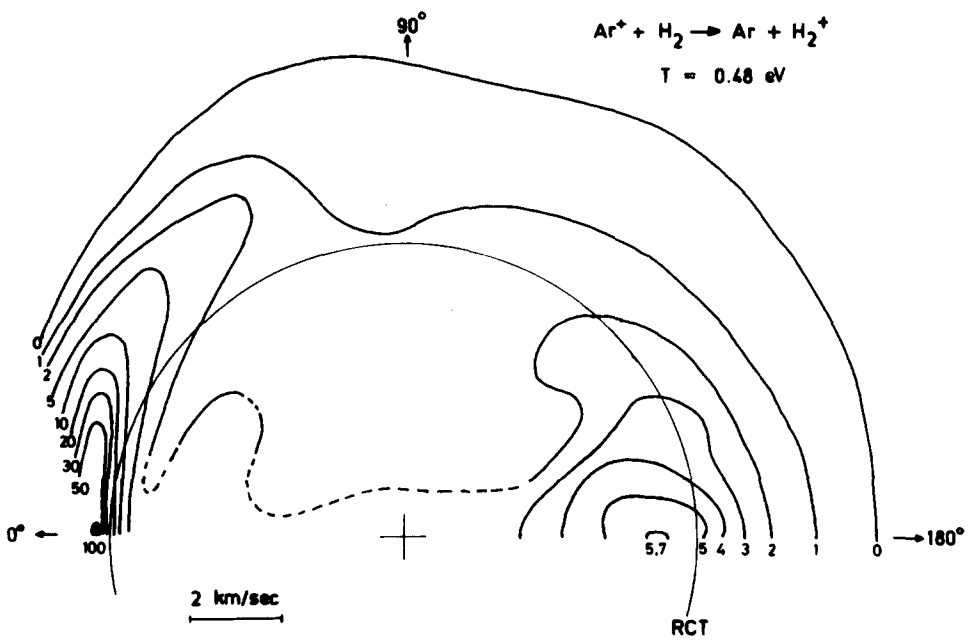


FIG. 4. Scattering contour map for $H_2^+$ produced in reaction (1) at a relative collision energy of 0.48 eV (c.m.).

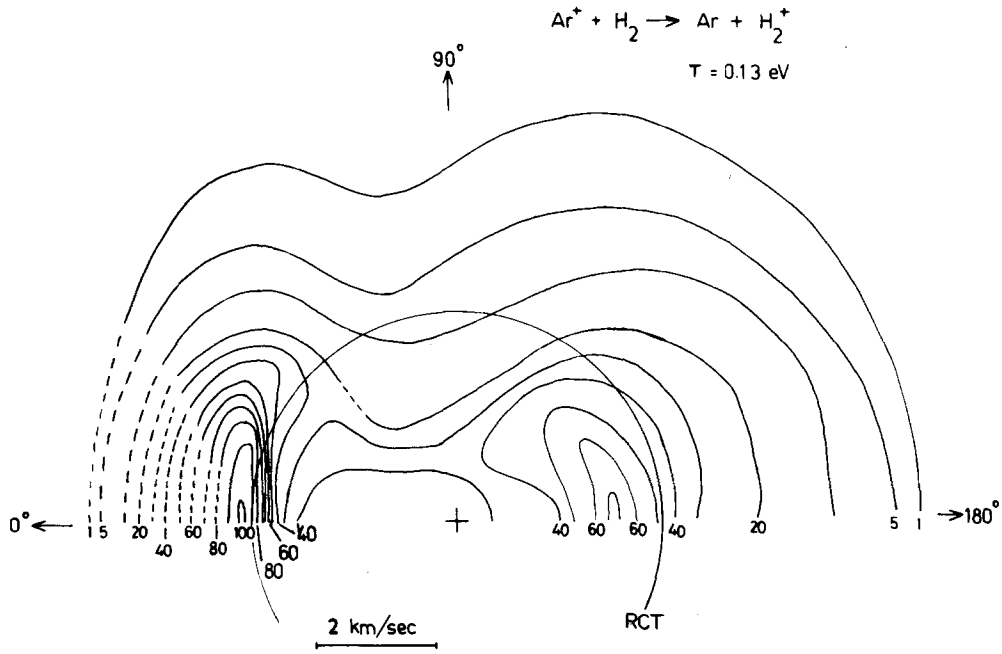


FIG. 5. Scattering contour map for $H_2^+$ produced in reaction (1) at a relative collision energy of 0.13 eV (c.m.).

derived from the contour maps using the relation

$$I(\chi) = \int_0^\infty u^2 P_C(u, \chi)\, du \,, \tag{3}$$

where $P_C(u, \chi)$ is the Cartesian probability of finding product at the c.m. velocity $u$ and scattering angle $\chi$. The results (Fig. 6) show a strong, narrow peak in the forward ($\chi = 0°$) direction at all three energies. The fact that the product $H_2^+$ ions undergo little or no angular deflection indicates that charge transfer occurs by a simple electron jump at large intermolecular separation, as postulated in the rectilinear trajectory model[27] of charge transfer. Clearly, this is the vastly dominant mechanism at 3.44 eV, in agreement with Tully's trajectory calculations.[20]

$H_2^+$ ions scattered through large angles are presumably produced in intimate encounters resulting from small impact parameter collisions. Of little or no importance at the highest collision energy, this intimate collision mechanism is seen to be comparable in importance to the electron-jump mechanism at $T = 0.13$ eV. At this energy, the amount of $H_2^+$ scattered through large angles shows that charge transfer competes effectively with atomic rearrangement in small impact parameter collisions. The reported[22,23] decrease in the cross section for the charge transfer process, reaction (1), at low collision energies had been rationalized by the assumption[6] that atomic rearrangement, reaction (2), dominates in all collisions occuring with impact parameters less than the critical (Langevin) impact parameter for classical orbiting in an ion-induced dipole potential. The present results refute the validity of this assumption and indicate that a model such as that proposed by Wolf and Turner[28] might actually provide a more accurate description of charge transfer cross sections at low collision energies. These results also suggest the possibility that the observed decrease in the cross section for charge transfer might simply be an experimental artifact caused by low detection efficiency for $H_2^+$ ions scattered with high velocity throughout a large solid angle.

At high collision energies, however, large-angle scattering of $H_2^+$ is almost absent. Because the cross section for chemical reaction is also quite small at high energy, a large fraction of the small impact parameter collisions must result in elastic scattering, the abundant occurrence of which has been observed by Chiang *et al.*[16] over this energy range.

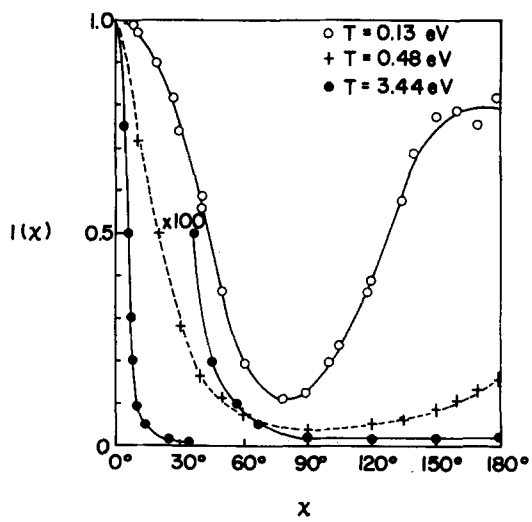


FIG. 6. Center-of-mass angular distribution $I(\chi)$ vs center-of-mass scattering angle $\chi$ for $H_2^+$ produced in reaction (1) at the relative collision energies of 0.13, 0.48, and 3.44 eV.

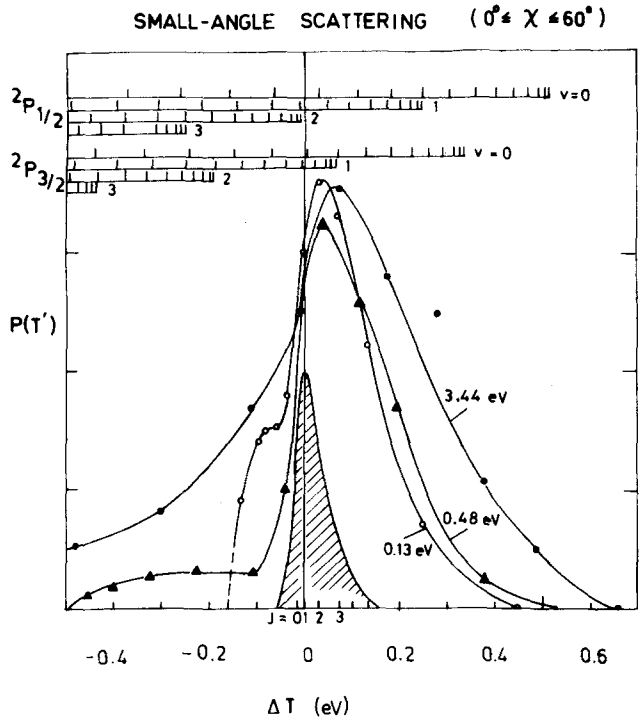


FIG. 7. Product translational energy distribution $P(T')$ for $H_2^+$ scattered through c.m. angles less than 60° (electron-jump mechanism), vs $\Delta T$, the change in relative translational energy ("translational exoergicity") of the system. The vertical line at $\Delta T = 0$ corresponds to resonant charge transfer. The lines at the top of the figure indicate the values of $\Delta T$ corresponding to the production of $H_2^+$ in particular vibrational and rotational states from $Ar^+$ in either the $^2P_{3/2}$ or the $^2P_{1/2}$ state. The shaded curve shows the distribution of relative collision energies for the experiment at $T = 0.13$ eV. The open circles present the data for the experiment at $T = 0.13$ eV, the solid triangles, for $T = 0.48$ eV, and the closed circles for $T = 3.44$ eV. The solid lines are smooth curves connecting the data points for a given experiment.

### C. Product translational energy distributions

Information on energy disposal in the reaction and on the final state population of the reaction product can be obtained from the distribution of product relative translational energy $P(T')$. For each experiment the translational energy distributions for the electron-jump mechanism and for the intimate collision mechanism were derived separately by appropriate three-dimensional intergration of the product contour maps over the regions $0° \leq \chi \leq 60°$ and $60° \leq \chi \leq 180°$, respectively. The results for the electron-jump mechanism are shown in Fig. 7, where $P(T')$ is plotted versus $\Delta T$, the change in relative translational energy of the system. The vertical line at $\Delta T = 0$ corresponds to resonant charge transfer, while positive values of $\Delta T$ indicate the conversion of internal to translational energy (i.e., an exothermic process), while negative values of $\Delta T$ indicate the converse. The lines at the top of the figure indicate the values of $\Delta T$ corresponding to the production of $H_2^+$ in particular vibrational and rotational states from $Ar^+$, in either the $^2P_{3/2}$ or the $^2P_{1/2}$ state. The shaded curve shows the distribution of relative collision energies for the experiment at $T = 0.13$ eV. This curve, which includes the thermal spread in the translational and rotational energies of $H_2$ as well as the spread in the translational energy of the $Ar^+$ ion beam, gives a measure of the energy resolution of the experiment.

The upper curves show the product translational energy distributions obtained for the electron-jump mechanism at the various collision energies. Four conclusions can be derived from these data. (i) The product energy distributions are remarkably similar despite the difference in collision energy, indicating that the distribution of $H_2^+$ internal states produced by the electron-jump mechanism is rather insensitive to the collision energy. (ii) In all cases the maximum in the distributions occur just on the exothermic side of the RCT line, indicating the release of a small amount (0.07 eV) of internal energy as product translation. Unfortunately, the present experiment cannot provide direct information on the partitioning of product excitation between vibrational and rotational modes, so some ambiguity exists concerning the exact $v'$, $J'$ state of $H_2^+$ formed. There is, however, evidence from studies of similar charge transfer reactions that large values of $\Delta J$ are very unlikely.[29] Assuming this to be the case, the data show that $H_2^+$ is most likely to be formed with $v' = 1$ form $Ar^+(^2P_{3/2})$ and with $v' = 2$ from $Ar^+(^2P_{1/2})$, $J'$ being small in both cases. Because much of the width of the product translational energy distributions is caused simply by the spread in the initial collision energy, we can also conclude (iii) that exothermic processes ($v' = 0$) are rather unlikely, and (iv) that endothermic processes are very unlikely in the electron-jump mechanism.

The importance of Franck–Condon (FC) factors and energy resonance on the magnitude of charge transfer rate constants is a question that has often been raised in the literature but has not yet been resolved.[29] In an effort to shed some light on this important problem, we have analyzed the product translational energy distributions for the electron-jump mechanism in some detail, using models that focus on each of these factors.

The basic assumption of the first model (hereafter referred to as the FC model) is that the probability of forming $H_2^+$ in a particular vibrational state $v'$ is determined by the FC factor for the transition to that state from the ground vibrational state of $H_2$, subject only to the condition that the state $v'$ is energetically accessible. The physical basis of this model is the supposition that, in the electron-jump mechanism, charge transfer is a fast process which takes place at large ion-molecule separations and on a time scale short compared to nuclear motion.

The second model considered (hereafter called the adiabatic model) assumes that the probability of forming $H_2^+(v')$ is unity for the vibrational state of $H_2^+$ most nearly resonant with the recombination energy (RE) of $Ar^+$ and is zero for other vibrational states of $H_2^+$. This assumption is consistent both with the empirical expression derived by Hasted[31,32] to fit charge transfer cross section data, and with semiclassical impact parameter calculations.[27,33] Hasted[31] found an exponential decrease in the cross section with an increase in the absolute value of the energy defect, while the calcula-

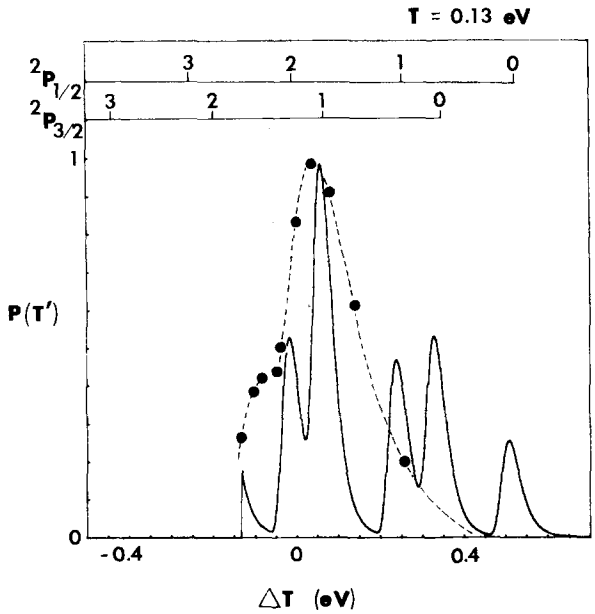


FIG. 8. Product translational energy distribution $P(T')$ for the electron-jump mechanism vs $\Delta T$, the change in relative translational energy, for the experiment at 0.13 eV relative energy. The solid line is the distribution predicted on the assumption that the probability of forming $H_2^+(v')$ is proportional to the Franck–Condon factor for the transition to $H_2^+(v')$ from the ground state of $H_2$. The solid circles represent the experimental data, and the broken line simply connects the data points.

tions by Rapp and Francis[27] indicate that the cross section varies inversely with $\Delta E$ to the fourth power at low velocities. The result obtained using either expression is that only the vibrational state of $H_2^+$ most nearly resonant with the RE of the reactant ion could be expected to make any significant contribution to the charge transfer process. (Rigorously, one should perhaps consider only the vibrational–rotational level of $H_2^+$ most nearly resonant with the RE of $Ar^+$.[32] As shown in Fig. 1, however, there exist in the present case vibrational states of $H_2^+$ which, in their ground rotational levels, are so nearly resonant with $Ar^+$ that the energy defect $\Delta E$ is less than the energy resolution of the experiment. As a result, the product translational energy distributions predicted by our adiabatic model are essentially the same if we consider the vibrational or the vibrational–rotational state of $H_2^+$ most nearly resonant with the RE of $Ar^+$. Consequently, we have ignored rotational sublevels in these model calculations.)

Two further assumptions, necessitated by experimental conditions, were common to both models: first, that the $Ar^+$ beam is a statistical 2:1 mixture of the $^2P_{3/2}$ and $^2P_{1/2}$ states, respectively; second, that (for lack of more precise information) the two states of $Ar^+$ have equal cross sections for charge transfer with $H_2$. The predicted product translational energy distributions, convoluted with the distribution of relative collision energies arising from the spread in $Ar^+$ and $H_2$ beam energies and the angular divergence of the $H_2$ beam, were then compared with the translational energy distributions obtained for the electron-jump mechanism at each of the three collision energies.

Figure 8 compares the predictions of the FC model with the product distribution measured in the experiment at 0.13 eV relative collision energy. The agreement is not particularly good, with the model predicting substantially more $H_2^+$ in the exothermic (low $v'$) channels than is observed experimentally. (The high $v'$ states of $H_2^+$ are, of course, energetically forbidden at this collision energy). In the 0.48 eV experiment (Fig. 9), the FC model also gives poor agreement, predicting appreciably more $H_2^+$ in both the exothermic and endothermic (high $v'$) channels than is measured. In the 3.44 eV experiment (Fig. 10), the FC model again overestimates the importance of the endothermic channels but gives reasonable agreement for the exothermic channels. From these comparisons we conclude that, particularly at the lower collision energies, the existence of favorable FC factors alone is not a sufficient condition for the product via the electron-jump mechanism of $H_2^+$ in vibrational states which are not nearly resonant with the RE of the reactant ion. This result is not unexpected, as it is generally recognized that the conversion of electronic energy into translational energy is rather inefficient.

Comparison of the adiabatic model with the measured product translational energy distribution for the electron-jump mechanism at 0.13 eV relative collision energy is shown in Fig. 11. Agreement, although not perfect, is considerably better than that obtained for the FC model (Fig. 8). Agreement between experiment and the adiabatic model is also found to be quite good for the $T = 0.48$ eV experiment (Fig. 12). The fact that the measured distributions are slightly broader than the predicted distributions in both cases may be attributed to experimental uncertainty in deriving the energy dis-

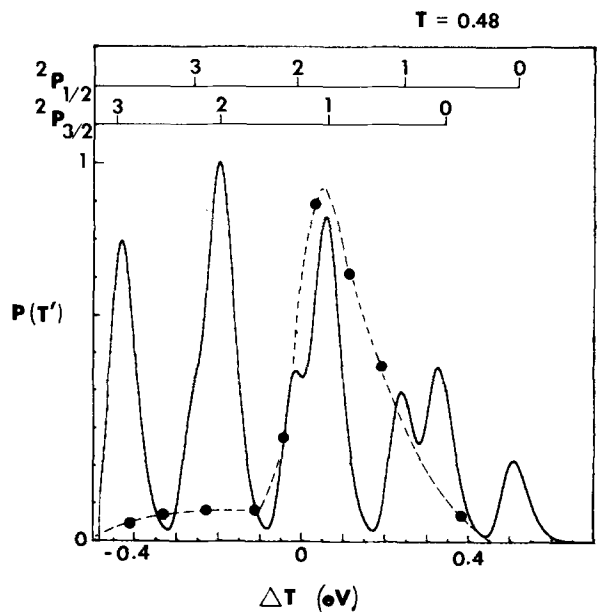


FIG. 9. Comparison of the observed product translational energy distribution for the electron-jump mechanism (broken line) with that predicted by the FC model (solid line) at $T = 0.48$ eV.

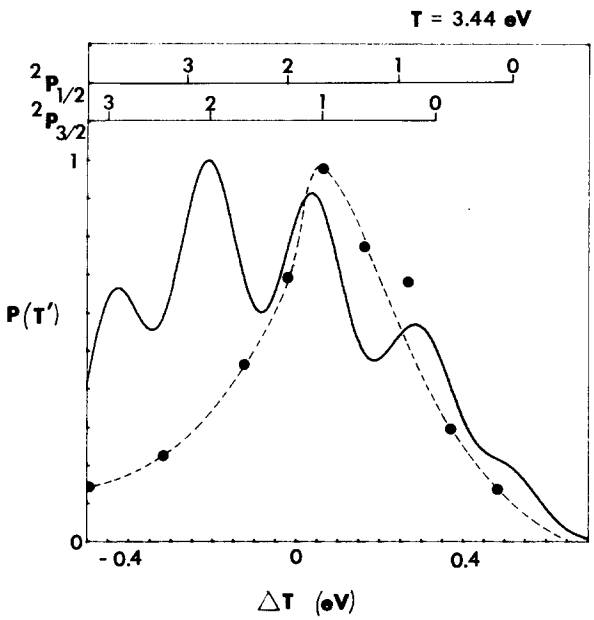


FIG. 10. Comparison of the observed product translational energy distribution for the electron-jump mechanism (broken line) with that predicted by the FC model (solid line) at $T$ = 3.44 eV.

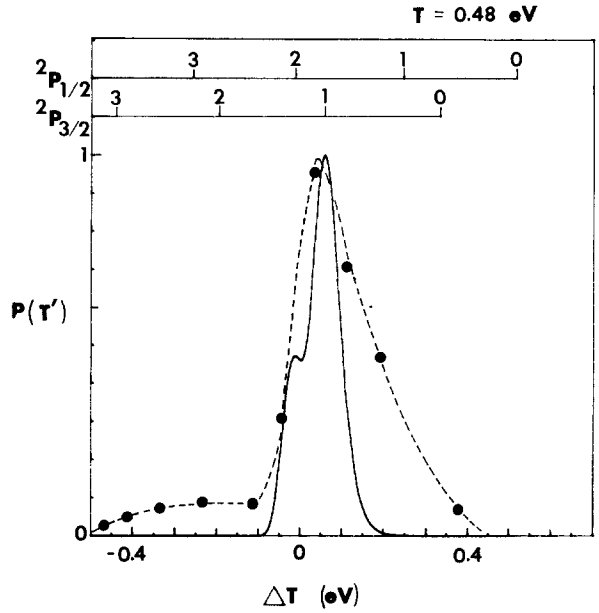


FIG. 12. Comparison of the observed product translational energy distribution for the electron-jump mechanism (broken line) with that predicted by the adiabatic model (solid line) at $T$ = 0.48 eV.

tributions from the contour maps and/or to changes in the rotational energy of the hydrogen in the charge transfer process. In the high-energy experiment (Fig. 13) agreement is less good, with the observed energy distribution being significantly broader than the predicted one. From these comparisons we conclude that, particularly at the lower collision energies, the electron-jump mechanism selectively populates that vibrational state of the molecular ion which is most nearly resonant with the RE of the reactant ion.

The product translational energy distributions produced by the intimate collision mechanism are shown in Fig. 14. Because the product energies varied considerably in the three experiments, the results are plotted separately as $P(T')$ vs $T'$. Again, the vertical

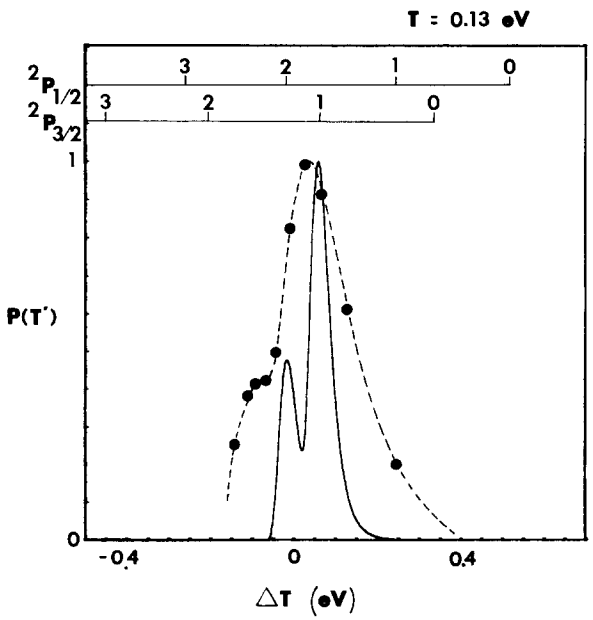


FIG. 11. Product translational energy distribution $P(T')$ for the electron-jump mechanism vs $\Delta T$, the change in relative translational energy, for the experiment at 0.13 eV relative energy. The solid line is the distribution predicted on the assumption that charge transfer exclusively produces the vibrational state of $H_2^+$ that is most nearly resonant with the recombination energy of the reactant ion (adiabatic model). The solid circles represent the experimental data, and the broken line simply connects that data point.

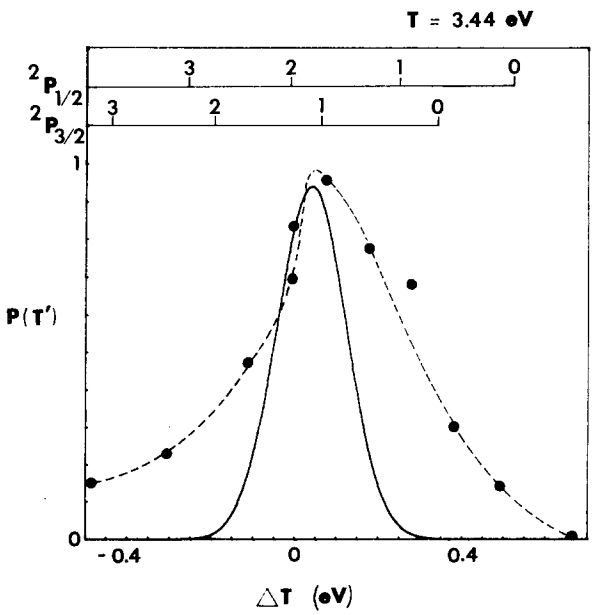


FIG. 13. Comparison of the observed product translational energy distribution for the electron-jump mechanism (broken line) with that predicted by the adiabatic model (solid line) at $T$ = 3.44 eV.

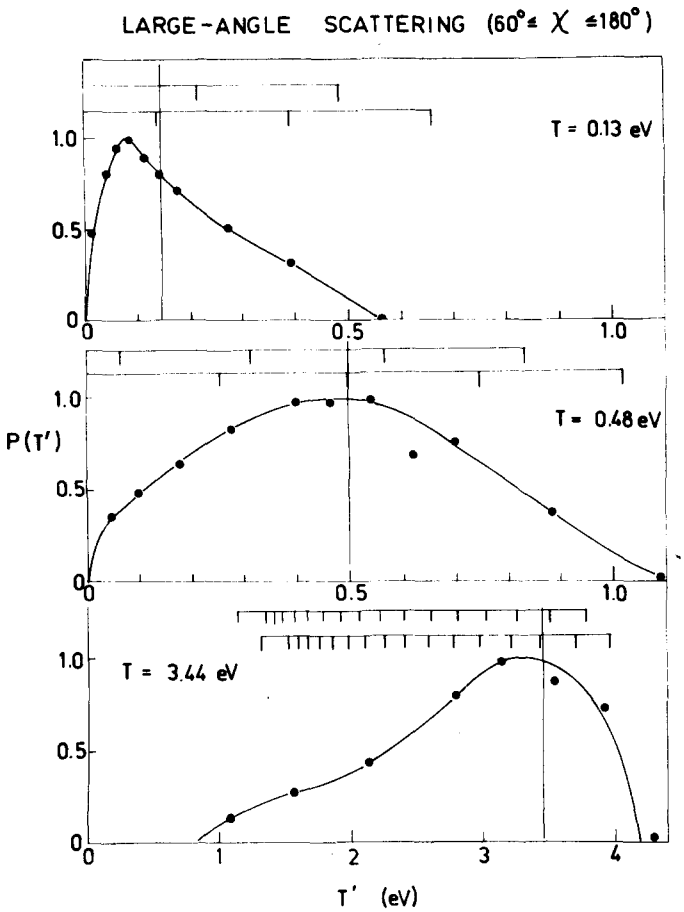


FIG. 14. Product translational energy distribution $P(T')$ vs $T'$ for $H_2^+$ scattered through c.m. angles greater than 60° (intimate collision mechanism). The upper figure presents the results for the experiment at $T = 0.13$ eV, the middle for $T = 0.48$, and the bottom for $T = 3.44$ eV. The long vertical line in each figure indicates the final translational energy expected from resonant charge transfer. The lines at the top of each section of the figure indicate the values of $T'$ corresponding to the formation of $H_2^+$ in various vibrational states (starting with $v = 0$ on the right) from $Ar^+$ in either the $^2P_{3/2}$ (upper line in each figure) or the $^2P_{1/2}$ (lower line) state.

line indicates the final translational energy expected from the resonant charge transfer process. The lines at the top of each figure, however, now indicate only the vibrational states of $H_2^+$ corresponding to a particular $T'$. These product energy distributions show three features in common. (i) They are very broad, indicating that $H_2^+$ is produced in a distribution of vibrational states by this mechanism. (ii) The distributions peak slightly to the endothermic side of the RCT line, indicating that the most probable mode of $H_2^+$ formation in intimate collisions involves the conversion of a small amount (~0.1 eV) of translational energy to internal energy of the ionic product. (iii) There is still appreciable product intensity at the point corresponding to conversion of all initial collision energy to product excitation. In fact, at $T = 3.44$ eV, some of the $H_2^+$ ions are excited to their dissociation limit. Presumably, dissociative charge transfer is also occurring at this collision energy, but no effort was made in the present study to detect the resulting $H^+$ ions.

## IV. SUMMARY

We have found that charge transfer between $Ar^+$ and $H_2$ proceeds in a direct manner rather than by the formation of a long-lived intermediate complex over the energy range 0.13–3.44 eV, and that two distinct reaction mechanisms are operative: (a) an electron jump at large separations occurs at all collision energies, and (b) an intimate collision mechanism becomes increasingly important as the collision energy is lowered. Secondly, the results show that electron transfer competes effectively with atomic rearrangement in small impact parameter collisions, particularly at the lower collision energies. Third, energy disposal depends upon the reaction mechanism: the electron-jump process produces a rather narrow distribution of internal states of $H_2^+$, with the most highly populated vibrational states of the product ion being those most nearly resonant with the recombination energy reactant ion. The intimate collisions, on the other hand, produce $H_2^+$ in a broad range of vibrational states, the most probable channels being those which are slightly endothermic.

*Visiting scientist under the auspices of the National Academy of Science (USA) and the Czechoslovak Academy of Sciences Scientific Exchange Program, 1976; Permanent address: Department of Chemistry, University of Kansas, Lawrence, KA 66045.

[1]J. F. Paulson, F. Dale, and S. A. Studniarz, Int. J. Mass Spectro. Ion. Phys. 5, 113 (1970).
[2]A. J. Masson, K. Birkinshaw, and M. J. Henchman, J. Chem. Phys. 50, 5412 (1969); A. J. Masson, Ph.D. Thesis, Brandeis University, 1970.
[3]E. W. Kaiser, A. Crow, and W. E. Falconer, J. Chem. Phys. 61, 2720 (1974).
[4]R. L. Champion and L. D. Doverspike, J. Chem. Phys. 49, 4321 (1968).
[5](a) Z. Herman, V. Pacăk, A. J. Yencha, and J. Futrell, Chem. Phys. Lett. 37, 329 (1976); (b) Z. Herman, V. Pacăk, and K. Birkinshaw, Presented at the Twenty-Third Annual Conference on Mass Spectrometry and Allied Topics, Houston, Texas, May 25–30, 1975.
[6]See, for example, G. R. North and J. J. Leventhal, J. Chem. Phys. 51, 4236 (1969), and E. A. Gislason, *ibid.* 57, 3396 (1972).
[7]D. P. Stevenson and D. O. Schissler, J. Chem. Phys. 29, 292 (1958).
[8]C. F. Giese and W. B. Maier II, J. Chem. Phys. 39, 439 (1963).
[9]F. S. Klein and L. Friedman, J. Chem. Phys. 41, 1789 (1964).
[10]K. Lacmann and A. Henglein, Ber. Bunsenges. Physik. Chem. 69, 286 (1965).
[11]A. Henglein, K. Lacmann, and B. Knoll, J. Chem. Phys. 43, 1048 (1965).
[12]Z. Herman, J. Kerstetter, T. L. Rose, and R. Wolfgang, Disc. Faraday Soc. 44, 123 (1966).
[13]L. D. Doverspike, R. L. Champion, and T. L. Bailey, J. Chem. Phys. 45, 4385 (1966).
[14]A. Ding, K. Lacmann, and A. Henglein, Ber. Bunsenges. Physik. Chem. 71, 596 (1967).
[15]R. D. Fink and J. S. King, J. Chem. Phys. 47, 1857 (1967).
[16]M. Chiang, E. A. Gislason, B. H. Mahan, C. W. Tsao, and A. S. Werner, J. Chem. Phys. 52, 2698 (1970).
[17]P. M. Hierl, Z. Herman, and R. Wolfgang, J. Chem. Phys. 53, 660 (1970).

[18]E. Teloy and D. Gerlich, Chem. Phys. 4, 417 (1974).
[19]T. F. Moran and P. C. Cosby, J. Chem. Phys. 51, 5724 (1969).
[20]J. Tully, Ber. Bunsenges. Physik. Chem. 77, 550 (1973).
[21]S. Chapman and R. K. Preston, J. Chem. Phys. 60, 650 (1974).
[22]R. C. Amme and J. F. McIlwain, J. Chem. Phys. 45, 1224 (1966).
[23]P. Mahadevan and G. D. Magnuson, Phys. Rev. 171, 103 (1968).
[24](a) G. Herzberg, *Spectra of Diatomic Molecules*, 2nd ed. (Van Nostrand, Princeton, N. J., 1950), p. 534; (b) L. Asbrink, Chem. Phys. Lett. 7, 549 (1970).
[25]J. L. Franklin, J. G. Dillard, H. M. Rosenstock, J. T. Herron, K. Draxl, and F. H. Field, *Ionization Potentials, Appearance Potentials, and Heats of Formation of Gaseous Positive Ions*, Nat. Stand. Ref. Ser., Nat. Bur. Stand. Circl. No. 26 (1969).
[26]Z. Herman and K. Birkinshaw, Ber. Bunsenges. Physik. Chem. 77, 566 (1973).
[27]D. Rapp and W. E. Francis, J. Chem. Phys. 37, 2631 (1962).
[28]F. A. Wolf and B. R. Turner, Abstract of the Vth I.C.P.E.A.C., Leningrad, 1967, p. 191.
[29]K. Birkinshaw and J. B. Hasted, J. Phys. B 4, 1711 (1971).
[30]See, for example, J. B. Laudenslager, W. T. Huntress, Jr., and M. T. Bowers, J. Chem. Phys. 61, 4600 (1974); and references cited therein.
[31]J. B. Hasted, J. Appl. Phys. 30, 25 (1959).
[32](a) D. K. Böhme, J. B. Hasted, and P. P. Ong, Chem. Phys. Lett. 1, 259 (1967); (b) J. Phys. B 1, 879 (1968).
[33]E. F. Gurnee and J. L. Magee, J. Chem. Phys. 26, 1237 (1957).